The catalytic conversion of CO_2 to hydrocarbons over Fe–K supported on Al_2O_3–MgO mixed oxides

Gurram Kishan, Myung-Woo Lee, Sang-Sung Nam, Myoung-Jae Choi and Kyu-Wan Lee *

Chemical Technology Division-I, Korea Research Institute of Chemical Technology, PO Box 107, Yusong, Taejon 305-600, Korea

Received 17 July 1998; accepted 10 November 1998

Al_2O_3–MgO mixed oxides prepared by a co-precipitation method have been used as supports for potassium-promoted iron catalysts for CO_2 hydrogenation to hydrocarbons. The catalysts have been characterized by XRD, BET surface area, CO_2 chemisorption, TPR and TPDC techniques. The CO_2 conversion, the total hydrocarbon selectivity, the selectivities of C_2–C_4 olefins and C_{5+} hydrocarbons are found to increase with increase in MgO content upto 20 wt% in Fe–K/Al_2O_3–MgO catalysts and to decrease above this MgO content. The TPR profiles of the catalysts containing pure Al_2O_3 and higher (above 20 wt%) MgO content are observed to contain only two peaks, corresponding to the reduction of Fe_2O_3 to Fe^0 through Fe_3O_4. However, the TPR profile of 20 wt% MgO catalyst exhibits three peaks, which indicate the formation of iron phase through FeO phase. The TPDC profiles show the formation of three types of carbide species on the catalysts during the reaction. These profiles are shifted towards high temperatures with increasing MgO content in the catalyst. The activities of the catalysts are correlated with physico-chemical characteristics of the catalysts.

Keywords: CO_2 hydrogenation, hydrocarbons, Al_2O_3–MgO, iron, potassium, TPR, TPDC

1. Introduction

The environmental impact of high concentrations of CO_2 in the atmosphere has been of acute concern to the global community [1,2]. One of the ways to mitigate this problem is to convert CO_2, at the generation point, to valuable industrial feedstocks such as lower olefins and liquid hydrocarbons [1–5]. Iron-based catalysts have shown great promise in reverse water–gas shift (RWGS) reaction as well as Fischer–Tropsch (F-T) synthesis, which are the two major steps involved in the hydrogenation of CO_2 [3–5]. However, the use of iron catalysts does not solve the problem of insufficient selectivity of industrially important lower olefins, which represents a general limitation of F-T synthesis. In order to overcome the limitations of Schulz–Flory product distribution, new support materials such as zeolites or modified metal oxides are used either to limit the chain growth by shape-selective effect or to intercept the molecular intermediates in the chain propagation sequence [6,7].

Potassium was found to be an effective promoter for iron-based catalysts in the F-T synthesis [8–10]. With the addition of potassium to an iron catalyst, production of light olefins and long-chain hydrocarbons is expected to be enhanced markedly. Lee and co-workers [3–5] have reported higher selectivities for the formation of lower olefins on unsupported Fe–K catalysts in the CO_2 hydrogenation. This selectivity enhancement was attributed to the formation of iron carbides on these catalysts [5,11]. On the other hand, several authors [12–14] emphasized the importance of support in iron catalysts for F-T synthesis, as it is expected to influence the iron particle size, reducibility, degree of interaction with the support and the chemical form of species present at the surface of the catalyst. Cagnoli et al. [14] reported that basic supports like MgO give improved selectivity to light olefins compared to Fe catalysts supported on typical materials such as SiO_2 and Al_2O_3 [12–14]. However, use of MgO alone as support can lead to poor dispersion. Gallegos et al. [13] have reported that iron supported on SiO_2–MgO gives good selectivity towards light olefins compared to iron supported either on SiO_2 or MgO in F-T synthesis.

In the present study, we have used Al_2O_3–MgO mixed oxides as supports for potassium-promoted iron catalysts in CO_2 hydrogenation. These catalysts have been characterized by XRD, BET surface area, TPR, TPDC and CO_2 chemisorption techniques. An attempt has also been made to correlate the results with hydrocarbon distribution in CO_2 hydrogenation.

2. Experimental procedure

The Al_2O_3–MgO mixed oxide supports were prepared by varying the proportion of Al_2O_3 and MgO by the co-precipitation method. These oxides were precipitated by adding aqueous ammonia to mixed solutions of aluminum nitrate and magnesium nitrate (final pH = 9.5). The gels were dried at 383 K for 16 h and calcined at 773 K for 8 h. Surface areas of these supports were around 200 $m^2\,g^{-1}$. Fe–K (10 wt% Fe) catalysts were prepared by depositing iron nitrate and potassium nitrate on the mixed oxide supports by the impregnation method. The atomic ratio of

---

* To whom correspondence should be addressed.

Fe : K is maintained as 2 : 1. The catalysts were dried and calcined at 773 K for 24 h.

Powder X-ray diffraction patterns of supports and catalysts were recorded using a Rigaku 2155D6 X-ray diffractrometer with nickel-filtered Cu Kα radiation.

Chemisorption of carbon dioxide was performed using a conventional high-vacuum volumetric chemisorption apparatus (Micromeritics, ASAP 2400) by the double-isotherm method [11] at 298 K. Prior to the adsorption measurements, the samples were reduced in a flow of hydrogen at 723 K for 16 h and the catalyst cell was evacuated and cooled to room temperature under dynamic vacuum ($<10^{-5}$ Torr).

For TPR studies, 50 mg of the calcined catalyst was loaded in a quartz reactor and heated at 673 K for 6 h under argon atmosphere. After cooling the sample to room temperature, a high-purity premixed gas containing 95% argon and 5% hydrogen was used as a reducing agent. TPR profiles were collected while the catalyst was heated linearly at 5 K/min. Traces of oxygen and water were removed by passing through an activated molecular sieve trap kept in an ice bath.

Prior to decarburization experiments, 200 mg of catalyst was reduced at 723 K in H_2 for 24 h. The reduced catalyst was exposed to H_2/CO_2 (3/1) mixed gas at 573 K and 1 atm for 4 h. After the reaction, the catalyst bed was quickly cooled down to room temperature in argon gas. Then argon was replaced by hydrogen gas and TPDC profiles were obtained while raising the temperature of the catalyst linearly to 973 K at 5 K/min. It was found that the product was almost exclusively methane (over 99%).

Hydrogenation of CO_2 was carried out in a fixed-bed flow reactor made of stainless steel (10 mm i.d. and 200 mm length). The particle size of the catalysts was maintained between 25 and 40 mesh. Prior to introducing the reactant gas mixture ($H_2/CO_2 = 3$) into the reactor, the catalyst was reduced in H_2 at 723 K for 24 h. The reaction was carried out at 573 K and at 10 atm pressure for 24 h. The gas transfer line from the reactor to gas chromatograph was heated at 423 K and a trap was also kept in the transfer line. The products were analyzed by an on-line gas chromatograph (Chrompak CP 9001) equipped with TCD (Porapak Q column) and FID (GS-Q capillary column) detectors.

3. Results and discussion

The BET surface areas of the catalysts are listed in table 1. The results indicate that the surface areas are decreasing gradually with increasing MgO content. In fact, the surface areas of the supports have been observed to follow a similar trend. However, the decrease was more profound after impregnation with iron and potassium, which may be attributed to pore blockage.

Table 1
BET surface area and CO_2 chemisorption values of Fe–K catalysts supported on Al_2O_3–MgO.

Catalyst	BET surface area (m^2/g)	CO_2 uptake (μmol/g)
Fe–K/Al_2O_3(100)	172.11	337.37
Fe–K/Al_2O_3(90)–MgO(10)	173.90	373.05
Fe–K/Al_2O_3(80)–MgO(20)	162.13	402.34
Fe–K/Al_2O_3(70)–MgO(30)	129.39	328.10
Fe–K/Al_2O_3(50)–MgO(50)	92.34	241.11
Fe–K/Al_2O_3(25)–MgO(75)	88.29	203.32
Fe–K/MgO(100)	25.67	50.14

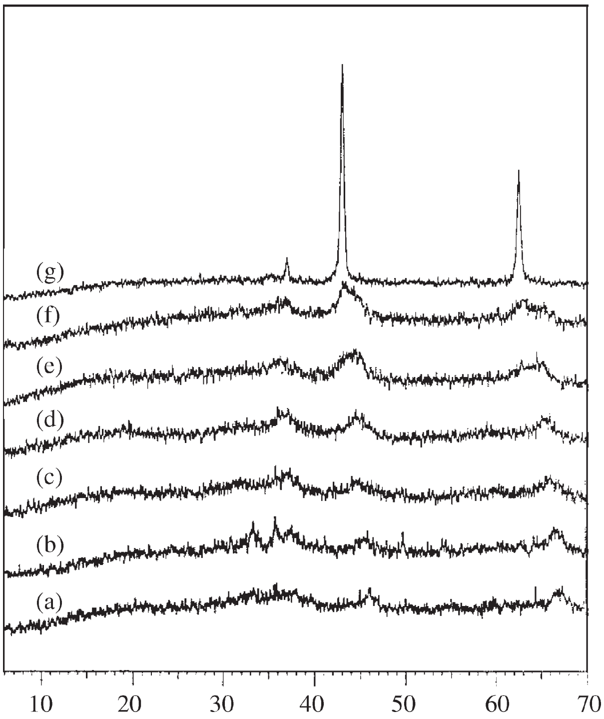

Figure 1. XRD patterns of 10 wt% Fe–K/Al_2O_3–MgO catalysts with different Al_2O_3–MgO proportions: (a) Al_2O_3, (b) Al_2O_3(90)–MgO(10), (c) Al_2O_3(80)–MgO(20), (d) Al_2O_3(70)–MgO(30), (e) Al_2O_3(50)–MgO(50), (f) Al_2O_3(25)–MgO(75), (g) MgO.

Figure 1 shows the XRD pattern of Fe–K catalysts supported on Al_2O_3–MgO mixed oxides with varying Al_2O_3 and MgO ratios. No XRD peaks corresponding to oxides of Fe and K have been observed in the samples, confirming that iron and potassium are well dispersed on the surface of the supports. However, for all the samples, peaks corresponding to supports have been clearly observed. Catalysts with pure Al_2O_3 and 90 wt% Al_2O_3 supports show peaks corresponding to γ-Al_2O_3. Its more intense peaks are at $2\theta = 45.8$ and 66.8° (figure 1), whereas peaks corresponding to MgO start appearing along with Al_2O_3 peaks from 20 wt% MgO in the catalysts. The intensity of these peaks ($2\theta = 36.85$, 42.76 and 62.07°) increased with increasing MgO content. MgO and Al_2O_3 can react and form spinel at 873 K provided they are in intimate contact [15]. In our case, XRD patterns reveal the absence of such a spinel. Taking into account that the calcination of the samples was performed at 773 K, the possibility of spinel formation does not exist.

Table 2

CO_2 hydrogenation[a] over Fe–K catalysts supported on mixed metal oxide (Al_2O_3–MgO).

	Catalyst (Fe–K) Al_2O_3 : MgO						
	100 : 0	90 : 10	80 : 20	70 : 30	50 : 50	25 : 75	0 : 100
CO_2 conv. (%)	21.34	24.05	27.53	23.08	18.79	16.83	13.75
Selectivity (C mol%)							
CO	38.65	26.20	18.57	37.98	53.39	59.33	79.80
–HC–	61.35	73.80	81.43	62.02	46.61	40.67	20.20
Hydrocarbon distribution (C mol%)							
C_1	30.42	28.34	22.92	26.08	27.76	33.27	51.58
$C_2^=$	2.47	2.77	4.89	8.80	8.75	7.27	1.96
C_2	16.44	15.76	10.52	9.51	8.79	12.85	23.97
$C_3^=$	10.33	12.16	15.93	18.21	14.24	11.37	6.04
C_3	9.59	9.21	5.92	4.60	7.13	8.47	9.49
$C_4^=$	7.50	10.92	14.65	5.01	10.20	6.99	3.20
C_4	7.10	4.70	4.47	11.84	5.31	6.93	1.11
C_{5+}	16.15	16.14	20.70	15.95	17.83	12.86	2.65
Selctivity of olefin (C_2–C_4) (C mol%)							
Ol./(Ol. + Para.)	38.00	46.56	62.91	55.24	61.00	47.58	24.47

[a] CO_2 hydrogenation at 1900 ml g^{-1} h^{-1}, 573 K, and 10 atm.

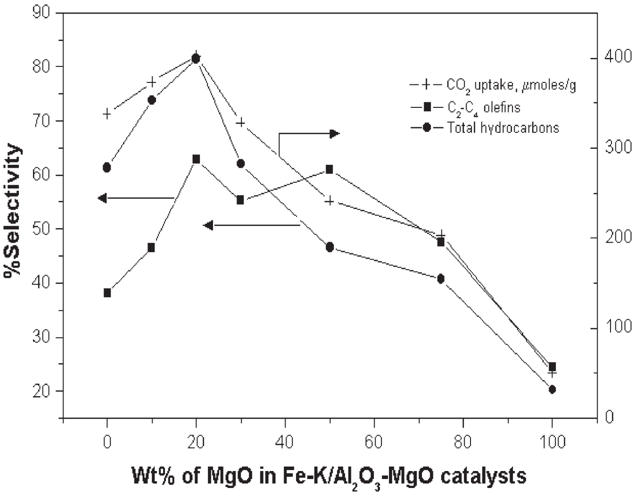

Figure 2. Dependence of total hydrocarbon, C_2–C_4 olefins selectivities, and CO_2 chemisorption over support composition in Fe–K/Al_2O_3–MgO catalysts.

The results of CO_2 hydrogenation to hydrocarbons are summarized in table 2. It is clear from table 2 that CO_2 conversion, selectivity to CO and total hydrocarbons vary based on support composition (figure 2). For all the catalysts, the conversion increased up to 12 h and remained constant. The reported data in table 2 corresponds to 24 h. The conversion of CO_2 and the total hydrocarbon content in products increased with increasing MgO content, peaking at 20 wt%, while further increase in MgO content of the support has an opposite effect. The selectivity towards C_2–C_4 olefins and C_{5+} hydrocarbons shows a similar trend. These results may be attributed to increase in the basicity of the catalysts, as revealed by the increasing CO_2 chemisorption with MgO content of the support. It is interesting to note that the selectivity towards methane falls initially with increasing MgO content reaching minimum at 20 wt% of MgO, while further increase in MgO content led to higher formation of methane. Dry and Oosthuizen [16] had also observed a decrease in methane selectivity with enhanced CO_2 chemisorption on alkali-promoted iron catalysts supported on SiO_2. In all the samples, the formation of C_3 and C_4 olefins is dominant compared to corresponding paraffins. However, the C_2 olefin content was found to be less when compared to corresponding paraffins.

According to Gallegos et al. [13], who studied the F-T synthesis over Fe/SiO_2–MgO catalysts, an optimal concentration of about 4 wt% of MgO offers the highest selectivity to olefins. Kemnitz et al. [17] have found the activity to increase upto 10% Mg in CCl_2F_2 dismutation reaction. Replacement of Al with Mg in γ-alumina results in a reduction of acid sites with weak and medium strength, whereas the strong acid sites may remain unchanged [18]. In the product distribution of the catalysts, there is a little deviation from the Anderson–Schulz–Flory (ASF) distribution. It might be due to either a limit to the chain growth probability or intercept of the molecular intermediates in the chain propagation sequence, in the presence of modified metal oxide supports [19]. Several authors [19–22] also reported a deviation in the Anderson–Schulz–Flory distribution, due to occurrence of some secondary reactions in the presence of zeolite supports. As has been observed, the increase in MgO content beyond 20 wt% results in the decrease of total hydrocarbon content. This behavior may be attributed to poor dispersion due to aggregation of iron particles on these supports. From these observations it is clear that bacisity of a catalyst alone may not be useful in the production of hydrocarbons from CO_2. Hence, the strong acid sites in conjunction with basic sites may be the real active sites responsible for the formation of hydrocarbons.

The CO_2 chemisorption results of the catalysts are shown in table 1. The CO_2 uptake values increased with increas-

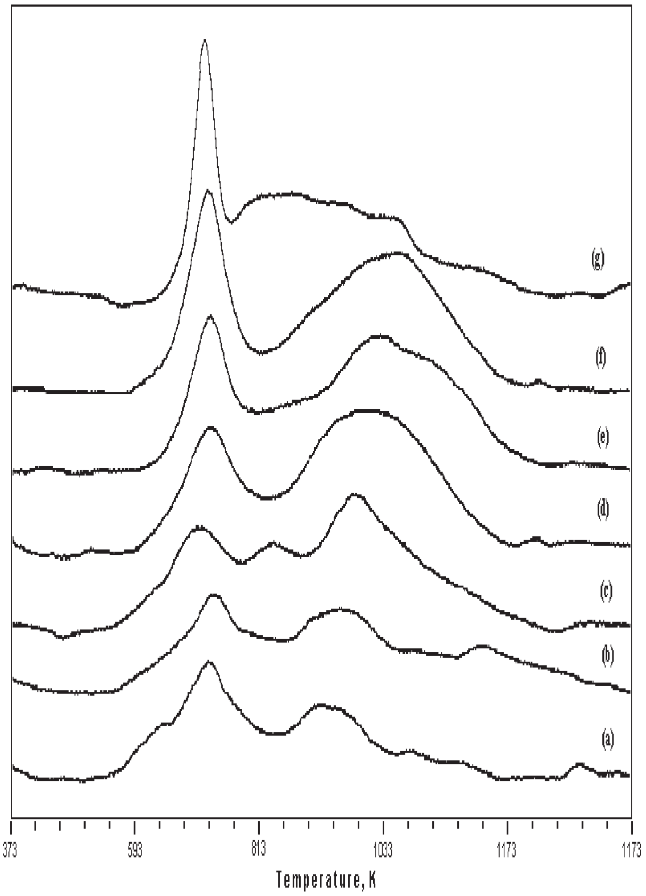

Figure 3. The TPR profiles of 10 wt% Fe–K/Al_2O_3–MgO catalysts with different Al_2O_3–MgO proportions: (a) Al_2O_3, (b) Al_2O_3(90)–MgO(10), (c) Al_2O_3(80)–MgO(20), (d) Al_2O_3(70)–MgO(30), (e) Al_2O_3(50)–MgO(50), (f) Al_2O_3(25)–MgO(75), (g) MgO.

ing MgO content up to 20 wt% in the catalysts, while further increase in MgO content led to a decrease. A good correlation was found between the CO_2 hydrogenation activity results and chemisorption uptakes (figure 2). It is evident from figure 2 that the total hydrocarbons and lower (C_2–C_4) olefins correlate with CO_2 uptakes. Even C_{5+} hydrocarbon selectivities were found to follow a similar trend.

The TPR profiles of Fe–K catalysts supported on Al_2O_3–MgO mixed oxides are shown in figure 3. They indicate a two- or three-stage reduction mechanism depending on the support composition. There is general agreement that the reduction of bulk-phase α-Fe_2O_3 proceeds in the following steps:

$$\underset{\text{haematite}}{\alpha\text{-}Fe_2O_3} \rightarrow \underset{\text{magnetite}}{Fe_3O_4} \rightarrow \underset{\text{wustite}}{FeO} \rightarrow \underset{\text{iron}}{\alpha\text{-}Fe}$$

The TPR profiles of Fe–K/Al_2O_3 catalysts show a two-stage reduction, the first step being at around 733 K and the second one at 945 K. It is the second peak which has shifted to higher temperatures with increasing MgO content in the catalyst. Usually, the first peak is attributed to reduction of Fe_2O_3 (haematite) to Fe_3O_4 (magnetite), whereas the second peak is attributed to reduction of Fe_3O_4 to Fe metal. We did not observe any peak corresponding to the formation of metastable FeO or Fe(II) aluminate. However, for the Fe–K/Al_2O_3(80)–MgO(20) catalyst, a three-stage reduction profile has been observed. The middle peak may be attributed to Fe_3O_4 to FeO transformation. Bulk-phase FeO is thermodynamically metastable compared to either magnetite or α-Fe at temperatures below 840 K [23]. However, in the presence of certain oxide supports, FeO may be stabilized and the stability of FeO on different oxide supports can be used to estimate the extent of the iron oxide–support interaction [24]. In this catalyst, there exists a strong interaction between surface iron oxide and mixed Al_2O_3(80)–MgO(20) oxide support. These results further support our observations in the CO_2 hydrogenation reaction. Yuan et al. [25] performed an *in situ* TPR and Mössbauer spectroscopy study over 10 wt% Fe/Al_2O_3 catalysts and observed a three-stage reduction mechanism. They interpreted the results as an indication of a strong metal (oxide)–support interaction in these catalysts and the TPR profile of their sample consisted of three consecutive stages [26]. In our studies, the height of the first reduction peak increased with increasing MgO content in the catalyst. This behavior may be due to the influence of MgO, which is a good electron donor, and hence it may have influenced the iron oxide making it more easy to reduce. Li et al. [27] had also observed that the main hydrogen-consuming peak shifted to low temperature (predominant peak) with increasing MgO content in Ru/Al_2O_3–MgO catalysts. Several authors [4,5] reported that the Fe_3O_4 phase is not favorable for CO_2 hydrogenation to hydrocarbons, whereas the iron carbides, which are reported to be active in CO_2 hydrogenation, have been speculated to be formed either from FeO or α-Fe. Our reaction results are in agreement with the TPR profiles.

Temperature-programmed decarburization (TPDC) profiles of Fe–K catalysts supported on Al_2O_3–MgO mixed oxides are shown in figure 4. All TPDC profiles show a single predominant peak with peak maximum temperature shifting from 800 to 973 K, when the MgO content in the catalyst support increased from 0 to 100. This shows that the stability of surface carbides increased with increasing MgO content. The amount of carbide increased with MgO content up to 20 wt% in Fe–K/Al_2O_3–MgO catalysts which further increase in MgO content led to its reduction and to decrease above this MgO content. For all the catalysts, two small broad humps were observed prior to the main peak and the areas of these peaks were highest for the Fe–K/Al_2O_3(80)–MgO(20) catalyst. These peaks may represent either the presence of other carbides with different stability or other decarburized pathway due to metal–support interaction. Barbier et al. [28] reported a relation between the selectivity and the extent of carbide formation in F-T synthesis over supported Ni catalysts. For our studies, also, the area of the main peak increased with increase in MgO content upto 20 wt% in the catalyst and decreased beyond this MgO loading. The formation of larger quantities of these carbides would increase the chain growth probability

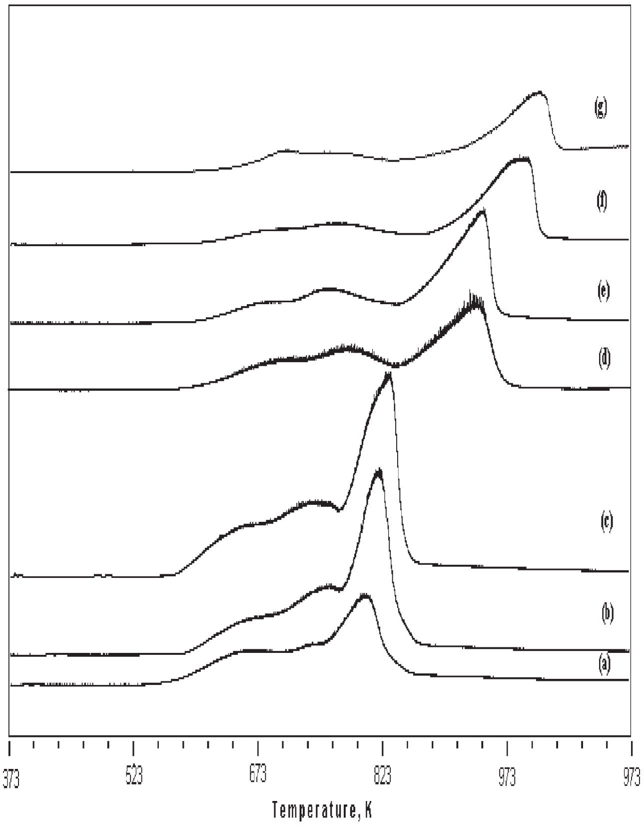

Figure 4. The TPDC profiles of 10 wt% Fe–K/Al_2O_3–MgO catalysts with different Al_2O_3–MgO proportions: (a) Al_2O_3, (b) Al_2O_3(90)–MgO(10), (c) Al_2O_3(80)–MgO(20), (d) Al_2O_3(70)–MgO(30), (e) Al_2O_3(50)–MgO(50), (f) Al_2O_3(25)–MgO(75), (g) MgO.

and increase the selectivity to olefins and C_{5+} hydrocarbons, as discussed in the activity results. The similarity between the TPR peaks, particularly the peak at 850 K, and the main TPDC peaks shows that a close relationship exists between the reduction of Fe_3O_4 to FeO, the formation of carbide structures and activity in CO_2 hydrogenation over these catalysts.

4. Conclusions

The results of an XRD study of the catalysts have revealed that iron and potassium are well dispersed over Al_2O_3–MgO mixed oxide supports. TPR of the catalysts shows that reduction of Fe_2O_3 to Fe^0 follows a two-step mechanism through Fe_3O_4. However, 20 wt% of MgO content in the catalyst resulted in stability of the metastable FeO peak, which shows a strong metal (oxide)–support interaction. The TPDC profiles of these catalysts shift to higher temperatures, which indicates the stability of the carbide species with increase in MgO content in the catalysts. The CO_2 conversion and total hydrocarbon selectivity increase with increase in MgO content in the catalysts upto 20 wt%, but decrease beyond this loading. The C_2–C_4 olefin selectivity and C_{5+} hydrocarbon selectivity are found to increase in the same way as CO_2 chemisorption and the area of TPDC peaks and the area of the TPR peak corresponding to reduction of Fe_3O_4 to FeO of the catalysts.

Acknowledgement

We thank the Ministry of Science and Technology and the Ministry of the Environment, Korea, for their financial support.

References

[1] Y. Shitaka, Shokubai (Catalyst) 33 (1991) 482 (in Japanese).
[2] B. Delmon, Appl. Catal. B 1 (1992) 139.
[3] M.D. Lee, J.F. Lee and C.S. Chang, Bull. Chem. Soc. Jpn. 62 (1989) 2756.
[4] M.D. Lee, J.F. Lee and C.S. Chang, Appl. Catal. 72 (1991) 267.
[5] J.F. Lee, W.S. Cheen and M.D. Lee, Canad. J. Chem. Eng. 70 (1992) 511.
[6] Th. Bein, G. Schmiester and P.A. Jacobs, J. Phys. Chem. 90 (1986) 4851.
[7] G. Boskovic, G. Vlajnic, E. Kis, P. Putanov, L. Guczi and K. Lazar, Ind. Eng. Chem. Res. 33 (1994) 2090.
[8] C.H. Kuei, J.F. Lee and M.D. Lee, Chem. Eng. Comm. 101 (1991) 77.
[9] A.P. Raje and B.H. Davis, Catal. Today 36 (1997) 335.
[10] P. Putanov, G. Boskovic, G. Vlajnic, E. Kis, K. Lazar and L. Guczi, J. Mol. Catal. 71 (1992) 81.
[11] P.-H. Choi, K.-W. Jun, S.-J. Lee, M.-J. Choi and K.-W. Lee, Catal. Lett. 40 (1996) 115.
[12] M.V. Cagnoli, S.G. Marchetti, N.G. Gallegos, A.M. Alvarez, R.C. Mercader and A.A. Yeramian, J. Catal. 123 (1990) 21.
[13] N.G. Gallegos, A.M. Alvarez, M.V. Cagnoli, J.F. Bengoa, S.G. Marchetti, R.C. Mercader and A.A. Yeramian, J. Catal. 161 (1996) 132.
[14] M.V. Cagnoli, S.G. Marchetti, N.G. Gallegos, A.M. Alvarez, A.A. Yeramian and R.C. Mercader, Mater. Chem. Phys. 27 (1991) 403.
[15] G.E. Vrieland, B. Khazai and C.B. Murchism, Appl. Catal. A 134 (1996) 123.
[16] M.E. Dry and G.J. Oosthuizen, J. Catal. 11 (1968) 18.
[17] E. Kemnitz, A. Hess, G. Rother and S. Troyanov, J. Catal. 159 (1996) 332.
[18] P. Berteau and B. Delmon, Catal. Today 7 (1989) 121.
[19] P.D. Caesar, J.A. Brennar, W.E. Garwood and J. Ciric, J. Catal. 56 (1979) 274.
[20] N.O. Egiebor, W.C. Cooper and B.W. Wojciechowski, Appl. Catal. 55 (1989) 47.
[21] N.O. Egiebor and W.C. Cooper, Appl. Catal. 14 (1985) 323.
[22] N.O. Egiebor, W.C. Cooper and B.W. Wojciechowski, Canad. J. Chem. Eng. 63 (1985) 826.
[23] A.J.H.M. Koch, H.M. Fortuin and J.W. Geos, J. Catal. 96 (1985) 261.
[24] X. Gao, J. Shen, Y. Hsia and Y. Chen, J. Chem. Soc. Faraday Trans. 89 (1993) 1079.
[25] T.R. Yuan, Z. Su, W. Chengyu, L. Dongbai and L. Liwu, J. Catal. 106 (1987) 440.
[26] I.R. Leith and M.G. Howden, Appl. Catal. 37 (1985) 75.
[27] Y. Li, S. Wu, P. Ying and Q. Xin, React. Kinet. Catal. Lett. 40 (1989) 53.
[28] A. Barbier, E.B. Perecia and G.A. Martin, Catal. Lett. 45 (1997) 221.